Langmuir

ARTICLE

pubs.acs.org/Langmuir

Characterization of Primary Amine Capped CdSe, ZnSe, and ZnS Quantum Dots by FT-IR: Determination of Surface Bonding Interaction and Identification of Selective Desorption

Jason K. Cooper, Alexandra M. Franco, Sheraz Gul, Carley Corrado, and Jin Z. Zhang*

Department of Chemistry and Biochemistry, University of California, Santa Cruz, Santa Cruz, California 95064, United States

ABSTRACT: Surface ligands of semiconductor quantum dots (QDs) critically influence their properties and functionalities. It is of strong interest to understand the structural characteristics of surface ligands and how they interact with the QDs. Three quantum dot (QD) systems (CdSe, ZnSe, and ZnS) with primary aliphatic amine capping ligands were characterized primarily by FT-IR spectroscopy as well as NMR, UV−vis, and fluorescence spectroscopy, and by transmission electron microscopy (TEM). Representative primary amines ranging from 8 to 16 carbons were examined in the vapor phase, KBr pellet, and neat and were compared to the QD samples. The strongest hydrogen-bonding effects of the adsorbed ligands were observed in CdSe QDs with the weakest observed in ZnS QDs. There was an observed splitting of the N−H scissoring mode from 1610 cm^{-1} in the neat sample to 1544 and 1635 cm^{-1} when bound to CdSe QDs, which had the largest splitting of this type. The splitting is attributed to amine ligands bound to either Cd or Se surface sites, respectively. The effect of exposure of the QDs dispersed in nonpolar medium to methanol as a crashing agent was also examined. In the CdSe system, the Cd-bound scissoring mode disappeared, possibly due to methanol replacing surface cadmium sites. The opposite was observed for ZnSe QDs, in which the Se-bound scissoring mode disappeared. It was concluded that surface coverage and ligand bonding partners could be characterized by FT-IR and that selective removal of surface ligands could be achieved through introduction of competitive binding interactions at the surface.

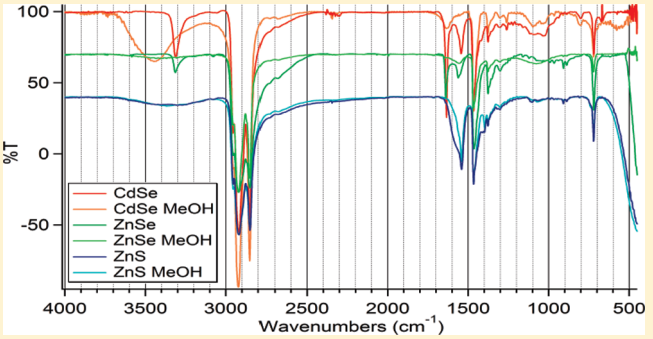

INTRODUCTION

Semiconducting nanomaterials such as nanocrystals (NCs) or quantum dots (QDs) have found useful applications in a wide range of fields from biology to materials science. Their successful development in applications such as fluorescence labeling of biomolecules,[1] light harvesting in quantum dot sensitized solar cells,[2−7] and photoelectrochemical cells[8−11] as well as next-generation lighting technologies, including quantum dot light emitting diodes (QD-LED's)[12−15] and alternating current driven electroluminescence,[16−18] have proven their broad range of usefulness in the scientific community. The unique properties observed in these materials are due to the small size of the particles; this gives rise to quantum confinement effects which are capitalized for tuning emission wavelengths. It is also a consequence of the small size that the particle properties can be dominated by the surface atoms, since the surface-to-volume ratio can be quite high compared to bulk. These surface effects can be influenced by surface defect sites, dangling bonds, or capping ligands; this study addresses the effects of the latter contributor.

Capping ligands are required to impart solubility and stability properties to the particles as well as to reduce aggregation. The effects of the capping ligand on the structural and electronic properties has been shown to be equally important.[19−24] Capping surface atoms of QDs with an organic ligand increases their coordination number to that of the internal atoms, thereby reducing dangling bond energy states within the band gap which can act as nonradiative emission centers. The chemical nature of the capping ligands, while not directly involved in the band structure of the semiconductor, can have a substantial effect on the growth characteristics[24−27] and optical properties[22,25] of the material. Common capping ligands that have been investigated in organic media have included trioctylphosphine oxide (TOPO), phosphonic acids, amines, thiols, and carboxylic acids. Many high-temperature organic synthetic techniques utilize metal alkylcarboxylates, and it is often assumed that the resulting capping ligand is the alkylcarboxylic acid. However, some proposed mechanisms for the growth of the crystals indicate the elimination of the carboxylic acid early on,[28] so it is unlikely to be observed at the particle surface unless additional acids are added to the reaction mixture. It is also common for synthetic techniques to include a primary amine as well, and this has been shown to aid in the growth of zinc chalcogenide QDs by activating the zinc carboxylate precursor;[29] it is also known that at high temperature the amine will combine with carboxyl groups

Received: April 7, 2011
Revised: June 1, 2011
Published: June 02, 2011

to form amides,[30] further eliminating the chance of observing an acid as the resultant ligand. In addition, computational studies have shown that primary amines have greater surface binding energy than carboxylic acids, though lower binding energy compared to TOPO and phosphonic acids.[20,31,32] However, primary amines have the advantage of more complete surface coverage—which can theoretically reach 100%—over TOPO (30% coverage) due to reduced steric effects.[33,34] In addition, the added van der Waals force between alkyl chains has been determined for alkyl thiol SAM layers on Au and was found to be between 0.8 and 1.8 kcal/mol per CH_2 group, which may help tip the energy minimization in favor of the primary amine.[35−37] As a result, primary amines have been observed at the surface of our quantum dots even with TOP and TOPO in solution. Therefore, we have focused on the primary amine in this study, as they will likely continue to play a beneficial role in the emerging field of QDs for solid state lighting and other applications.

In this work, three II−VI quantum dot systems were examined by FT-IR spectroscopy in an effort to better understand the local environment of the ligand on the QD surface. Techniques like NMR are, of course, highly sensitive to local environment; however, the headgroup of the organic molecule attached to the quantum dot can be difficult or impossible to observe in the ^{1}H NMR due to peak broadening and shifting. While FT-IR is less sensitive to local chemical environment, it has, however, proven a powerful tool in characterization of the bonding between the ligand and the QD.[38] The three QDs studied were CdSe, ZnSe, and ZnS, all of which were capped with a long chain (C8−C18) aliphatic primary amine. The spectra did not appear to depend on the chain length over the range studied. As QD preparations commonly use a crashing step to help clean and isolate the particles from the crude reaction mixture, samples were collected immediately after this step and compared to the uncrashed sample to observe the effect of this step on surface interactions. The results demonstrate that surface coverage and ligand structure can be characterized by FT-IR and that selective removal of surface ligands can be achieved through the introduction of competitive binding interactions at the surface.

EXPERIMENTAL SECTION

Synthesis of CdSe−Hexadecylamine Quantum Dots. The CdSe QDs were synthesized under Ar protection using the hot injection method. A 50 mL three-neck round-bottom flask was charged with 10 g of ODE and 0.136 g of cadmium stearate and was degassed three times to a pressure of 150 mmHg for a total of 30 min with purging. The mixture was heated to 90 °C where it was degassed again for 10 min. The mixture was heated to 300 °C, where at which point a mixture of 0.039 g of Se, 2.5 g of TOP, and 0.2 g of HDA prepared under N_2 was injected into the stirring cadmium solution. Growth was continued until the exciton had red-shifted to 603 nm, as monitored by UV−vis, for a total reaction time of approximately 6−8 min. The mixture was cooled into room temperature where the crude reaction mixture was cleaned with the following procedure.

Synthesis of ZnSe−Hexadecylamine Quantum Dots. The synthesis of the ZnSe QDs was performed under Ar protection using the hot injection method. To begin, 0.06 g of zinc stearate with 10 mL of ODE was charged in a three-neck round-bottom flask. The mixture was evacuated to 150 mmHg three times for a total of 30 min with purging, with an additional evacuation at 90 °C for 15 min. The mixture was heated to 300 °C with stirring, at which point 0.032 g of Se powder dissolved in 0.32 g of TBP with 0.15 g of HDA and 1 mL of ODE was injected rapidly. Growth was continued at 250 °C until the first exciton had shifted to between 400 and 405 nm, as monitored by UV−vis spectroscopy. The solution was cooled to room temperature, after which QDs were separated from the crude reaction mixture with the reported cleaning procedure.

Synthesis of ZnS−Octadecylamine Quantum Dots. Synthesis of ZnS QDs was performed using the hot injection method under Ar protection. A 50 mL three-neck round-bottom flask was charged with 10 mL of ODE and 0.0597 g of zinc stearate. The solution was degassed three times to 150 mmHg for a total of 30 min with purging and then heated to 90 °C and degassed again for 10 min to 150 mmHg. The mixture was heated to 300 °C, at which point a mixture of 0.013 g of sulfur, 0.32 g of TBP, and 0.1 g of ODA prepared under N_2 and diluted in 0.6−1 mL of ODE was injected with stirring. The temperature was decreased to 250−260 °C where the growth was continued for 6 min before the reaction was cooled to room temperature and cleaned as described.

Cleaning of the QDs. To the crude reaction mixture, 2 mL of dichloromethane (DCM) mixed in 10 mL of methanol was added and mixed thoroughly. Separation of the methanol phase was encouraged through centrifugation, and the resulting MeOH layer was discarded. This process was repeated a minimum of three times until this layer was clear. To the resulting solution, acetone was added until the mixture became turbid, and the precipitate of the QDs was collected via centrifugation. The crystals were washed two times with acetone and collected by centrifugation, dried under Ar, and redispersed in a mixture of hexanes and DCM or toluene. This sample was then degassed with Ar and stored for 24 h prior to sample analysis. The sample was subsequently sampled for FT-IR, TEM, UV−vis, and PL measurements. The prepared samples dispersed in the nonpolar solvent were then crashed using methanol and then centrifuged to collect the final quantum dot precipitate. These were again redissolved in toluene or hexanes and sampled for FT-IR analysis.

FT-IR Sample Preparation and Characterization. All KBr . pellets were prepared using KBr which was stored at 120 °C and were ground in a N_2 glovebox to reduce any water and CO_2 contamination. Ground samples were sealed in small dry vials and stored in a desiccator until pressed into a pellet with a pellet press which was also stored in a desiccator. Samples were exposed to atmosphere for no more than 2 min before the spectra were collected. Neat samples were collected between NaCl windows prepared in a N_2 glovebox and stored under N_2 until analysis. The primary amine samples used as reference were generated by heating the respective compound in a septum-topped vial to 120−140 °C for 10 min while bubbling N_2. These samples were subsequently stored in a N_2 glovebox as well. The gas phase spectrum was collected using a gas cell with NaCl windows by placing a few drops of the heat-treated octylamine into the chamber in the N_2 glovebox. All spectra were collected at atmospheric pressure under mild heating of the sample cell.

QD samples were dispersed in either hexane or toluene and added dropwise to the top of a NaCl window under a mild stream of Ar. When a sufficient amount had been added to create the thin film and allowed to dry, the windows were placed into the vacuum transfer chamber of a N_2 glovebox and evacuated to ∼100 mmHg for 5 min to remove any remaining solvent. The transfer chamber was subsequently purged with N_2, and the windows were immediately placed into a desiccator for no more than 30 min before the spectra were collected.

Instrumentation. Absorption and photoluminescence spectra were collected at room temperature with a Hewlett-Packard 845A diode array UV−vis spectrometer and a Perkin-Elmer Luminescence spectrometer LS50B, respectively. ^{1}H and ^{13}C NMR were collected in d_6-benzene using a Varian Inova 600 NMR. Vibration spectra were recorded with a Perkin-Elmer FTIR spectrometer at a resolution of 4 cm^{-1}. TEM measurements were made using a JEOL JEM-1200EX microscope.

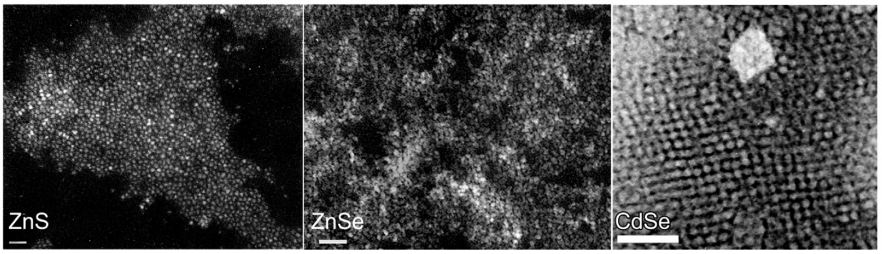

Figure 1. Representative images of the three quantum dot systems studied: (a) ZnS, (b) ZnSe, and (c) CdSe. Scale bar: 30 nm.

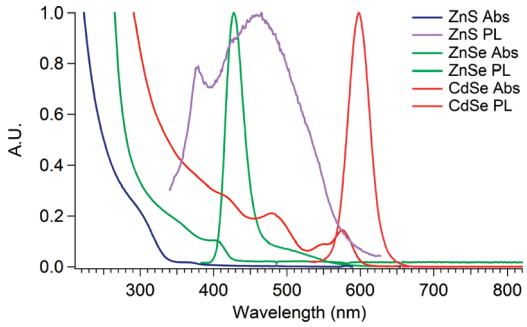

Figure 2. Absorption and emission spectra of ZnS (blue/purple), ZnSe (dark green/green), and CdSe (dark red/red).

RESULTS AND DISCUSSION

TEM, UV−vis, and Photoluminescence. All QD samples were prepared under similar conditions using organic solvents and the hot injection method as previously described. The samples were characterized using transmission electron microscopy (TEM). Figure 1 shows representative TEM images of different QD samples. The images indicate the presence of uniform nanospheres with monodispersity within 10% of the mean size distribution in all cases. The sizes of the QDs from TEM images were found to be approximately 4, 6, and 4 nm in diameter for ZnS, ZnSe, and CdSe, respectively. Since the excitonic position in the UV−vis absorption spectrum is dependent on particle size, it can be used to estimate the particle size. For example, for the CdSe QDs, a diameter of 3.8 nm was calculated based on the first excitonic peak observed in the UV−vis spectrum, which agrees closely with the TEM analysis (4 nm).[39]

Figure 2 shows UV−vis electronic absorption and photoluminescence spectra of the samples. The spectra are normalized to better compare the different samples. The CdSe QDs show a first exciton at 576 nm (2.15 eV). This energy is close to the bandgap energy of the QDs (differing by the small exciton binding energy) and suggests, when compared to the bulk band gap of 1.71 eV, that quantum confinement effects are important for the QDs. A Stokes shift of 0.08 eV was observed in the emission peak at 598 nm, which had a full width half-maximum (fwhm) of 34 nm. The shift has been implicated due to the electronic fine structure.[40,41] The narrow peak width is consistent with the monodispersity of the QDs determined by TEM analysis. The strong bandedge PL and weak trap state PL indicate a low density of trap states.[42,43]

The UV−vis spectrum of ZnSe QDs shows a first exciton peaked at 404 nm (3.07 eV). This is also larger than the bulk band gap of 2.69 eV for ZnSe, again indicating quantum confinement in the QDs. The PL spectrum shows a major emission band peak at 427 nm, which had a Stokes shift of 0.17 eV and a fwhm of 30 nm. There is a weak shoulder to the red of the main band-edge PL band that is apparently due to trap state emission. The narrow PL spectrum and weak trap state PL also suggest monodisperse QDS with low density of trap states.

For the ZnS QD sample, the first exciton appears at about 300 nm (4.13 eV), which is roughly the band gap energy and is larger compared to the bulk band gap energy of ZnS (3.68 eV), indicative of some quantum confinement effect. The PL spectrum exhibits two peaks at 378 and 459 nm which have a Stokes shift of 0.85 and 1.43 eV, respectively. The latter has been previously described as emission from vacancy states.[44]

NMR. While FT-IR analysis was sufficient to identify the capping ligand, further confirmation was achieved by ^{1}H and ^{13}C NMR. NMR has been successfully employed in characterization of alkylamines,[21,45,46] phosphonic acids,[47] carboxylic acids,[48] TOPO,[49] and thiophenol[50] capping ligands on QD surfaces, to name only a few. Shown in Figure 3a is the proton spectrum of hexadecylamine (color) and CdSe quantum dots with HDA capping ligands both in d_6-benzene (7.16 ppm).[51] Four peaks were observed at 0.51 ppm (br s), 0.92 ppm (t), 1.31 (m), and 2.53 ppm (t), corresponding to the amine, methyl, backbone, and α-hydrogens, respectively. In the CdSe sample, however, only two of these peaks remained from the amine; these were observed at 0.93 ppm (broad triplet) and 1.4 ppm (broad feature), with the remaining assigned peaks due to toluene contamination at 2.11 ppm (s) and 7.15 ppm (s). The additional peak at 0.30 ppm (s) is most likely due to a desorbed solution HDA species. The peaks from the α-C and the amine hydrogens interacting with the surface were not observed. The remaining backbone and methyl peaks were broadened which would result from the restricted motion of the surface bound ligands.

The ^{13}C NMR spectrum of the HDA in d_6-benzene (128.06 ppm) is reported as Figure 3b. The following peaks were observed and are reported with their carbon number assignments: C1 (42.7 ppm), C2 (34.5), C3 (27.4), C4−14 (30.2), C15 (23.1), and C16 (14.4). The following assignments were made for the QD-HDA sample: C1 (NA), C2 (34.3), C3 (27.3), C4−14 (30.2), C15 (23.2), C16 (14.4). The observation of the C1 carbon could not be resolved due to low S/N. A clear chemical shift was not observed for the HDA on the surface which is consistent with previous reports.[46] The result of the ^{1}H and ^{13}C NMR data confirm the capping ligand to be the aliphatic primary amine from the chemical shift data. The loss of the amine and alpha hydrogens confirm the QD surface interaction while peak broadening in both spectra is from reduced tumbling in solution.[46]

FT-IR of Primary Amines. As it was the goal of this investigation to use the vibrational spectra of primary amines on the surface of

dx.doi.org/10.1021/la201273x |*Langmuir* 2011, 27, 8486–8493

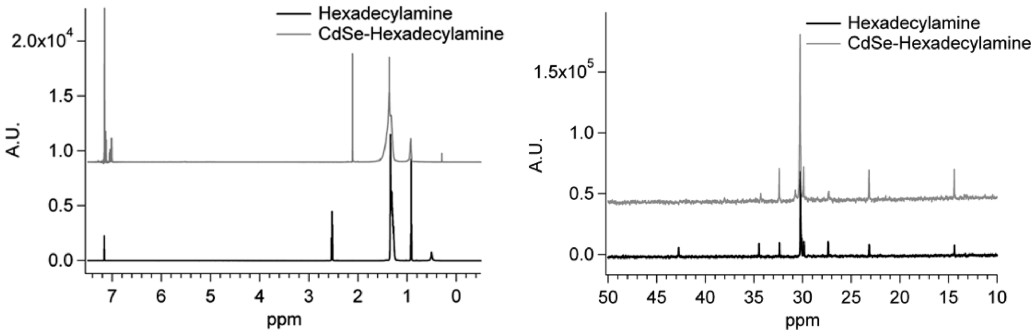

Figure 3. ^{1}H (left) and ^{13}C (right) NMR of hexadecylamine (black) and CdSe QD−hexadecylamine (gray) in d_6-benzene at 600 and 150.92 MHz, respectively.

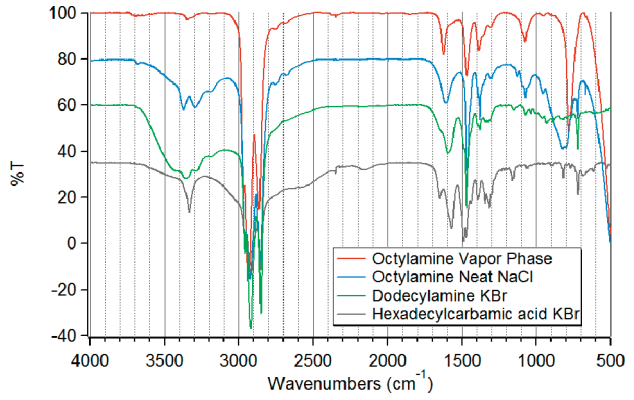

Figure 4. FT-IR spectrum from 500 to 4000 cm^{-1} of octylamine in the vapor phase (red), octylamine neat on NaCl (blue), dodecylamine in a KBr pellet (green), and hexadecylcarbamic acid in a KBr pellet (gray).

QDs to probe their structure and interaction with the QDs, it was necessary to first characterize the amines without the QDs as control experiments. Since the ligands bond through the NH_2 headgroup, changes in the N−H stretching and bending modes after bonding to the QD surface are expected. Therefore, adequate characterization of hydrogen-bonding effects was necessary. To accomplish this, the reference primary amines, octyl- and hexadecyl-, were examined and showed very similar spectral characteristics; however, some variability was observed dependent on the sample preparation. The samples were studied in various forms, including gas phase as well as neat on NaCl and in KBr pellet. The reference amine spectra are shown in Figure 4 for the full frequency range studied, 450−4000 cm^{-1}. In all spectra, it is not reasonable to compare intensities between samples because the exact molar concentrations and film thickness were impossible to correct for. Primary amines have been well characterized in the literature;[52−54] however, characterization is discussed here for the purpose of comparing to the quantum dot samples.

Beginning with the gas phase sample, for which octylamine was used (as longer chain amines had insufficient vapor pressures to provide adequate absorption), two weak NH_2 stretching peaks were observed at 3346 and 3316 cm^{-1}, corresponding to the antisymmetric and symmetric modes, respectively. However, free amines are expected to have stretching modes at 3496 and 3401 cm^{-1},[55,56] while bonded vapor phase ethylamine is expected to have stretching modes at 3344 and 3225 cm^{-1}.[52,57] The NH_2 scissoring mode was observed at 1623 cm^{-1} as a sharp peak with a fwhm of 13 cm^{-1}. The CH_2 bending modes were at 1467 and 1386 cm^{-1}. The broad peak at 1074 cm^{-1} was due to overlapping C−N stretching modes. Out-of-plane NH_2 bending was observed as a strong absorption at 781 cm^{-1} which eclipsed the backbone rocking mode expected at 722 cm^{-1}.

The neat octylamine spectrum showed a large increase in absorption in the N−H stretching region accompanied by spectral broadening, indicative of hydrogen bonding.[56] Three peaks could be identified at 3370, 3294, and 3191 cm^{-1}, the two former being N−H stretching modes and the latter being the overtone of the NH_2 bending mode interacting with the symmetric stretching mode.[56] The antisymmetric stretch was frequency upshifted by 24 cm^{-1} while the symmetric stretch was frequency downshifted by 22 cm^{-1} compared to that of the vapor phase amine. The NH_2 scissoring peak was located at 1609 cm^{-1}, which was downshifted by 14 cm^{-1} and was nearly triply broadened compared to the vapor phase sample, with a fwhm of 34 cm^{-1}. The C−H bending and C−N stretching modes were not shifted with respect to the vapor phase sample; however, the NH_2 out-of-plane bending was much broader, weaker, and slightly upshifted to 814 cm^{-1} allowing for observation of the C−H rocking peak at 723 cm^{-1}.

It should be noted that the hexadecylamine collected from the sample bottle that had been stored unprotected did not show the characteristic group frequencies for a primary amine. It is, however, well-known that primary amines will combine with CO_2 to form carbamic acids.[58−60] The FT-IR group frequencies did match a carbamic acid, as it showed a strong sharp peak at 3333 cm^{-1}, which is characteristic of carbamic acid compounds and is due to N−H stretching. This mode was observed over the top of a broad weak O−H stretch centered around the same frequency. Two peaks were observed at 1648 and 1568 cm^{-1} corresponding to the C═O stretching and NH_2 bending modes, respectively. This sample has therefore been assigned to hexadecylcarbamic acid; however, the spectrum of this compound has been occasionally miss-assigned in the literature as a primary amine. Consequentially, the primary amine was regenerated using the technique described in the Experimental Section. Adequate removal of any carbamic acids in the primary amine sample preparation by elimination of CO_2 via the degassing and heating method was supported by the absence of the sharp 3333 cm^{-1} peak in the N−H stretching region. As peaks were observed in a broad spectral region in the NH_2 scissoring mode and C═O stretching region, the N−H stretch was the only decisive peak for confirming the complete elimination of any carbamic acid.

dx.doi.org/10.1021/la201273x |*Langmuir* 2011, 27, 8486–8493

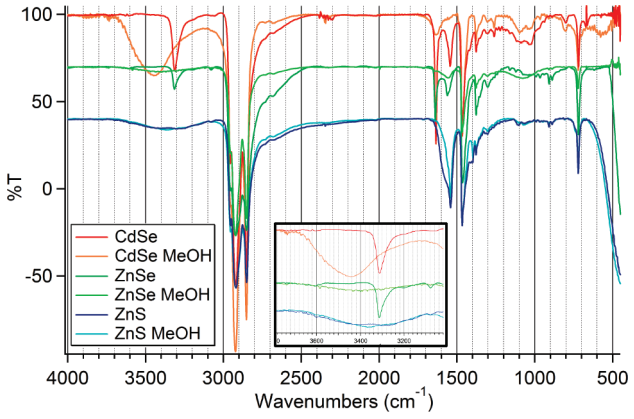

Figure 5. FT-IR spectrum from 500 to 4000 cm^{-1} of octadecylamine capped QD solid samples taken on NaCl plates before and after crashing with MeOH for CdSe (red/orange), ZnSe (green, light green), and ZnS (blue/light blue). Inset: expanded N−H stretching region from 3000 to 3800 cm^{-1}.

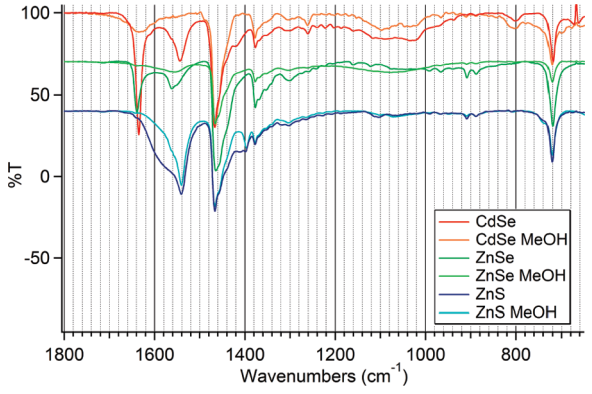

Figure 6. Expanded FT-IR spectrum from 730 to 1800 cm^{-1} of octadecylamine capped QD solid samples taken on NaCl plates before and after crashing with MeOH for CdSe (red/orange), ZnSe (green, light green), and ZnS (blue/light blue), highlighting the NH_2 scissoring region.

The hexadecylamine sample, which was ground and pressed in KBr, showed further broadening and shifting of the amine-related peaks. The N−H stretching peaks were further intensified and broadened with what could be identified as three peaks at 3357, 3283, and 3187 cm^{-1}. The NH_2 antisymmetric stretch was again upshifted by 11 cm^{-1} with respect to the vapor phase amine, while the symmetric stretch was downshifted by 33 cm^{-1}. The NH_2 scissoring mode was further downshifted to 1592 cm^{-1} and broadened, showing a shoulder at 1642 cm^{-1} which has been referred to by Randall et al. as "special invariant groups of unknown mode of vibration". It is our suggestion that the broadening and shifting observed in this region due to hydrogen bonding be evidence that the shoulder observed is due to "free" amines within the solid sample matrix. Also, the C−N stretch was weakened even further and the NH_2 out-of-plane stretch slightly upshifted over the neat sample and was also much diminished with some slight broadening.[61] In summary, hydrogen bonding effects were observed to increase from the vapor, liquid, and solid samples marked by increased NH stretching absorption and downshifting of the NH scissoring peak with broadening observed in both features.

FT-IR of Amines on Surface of QDs. *N−H Stretching Region.* With the free amines independently characterized, the vibration frequencies of the amines bound to the surface of QDs with emphasis on the changes were observed. The FT-IR spectra of octadecylamine capped QD samples of CdSe, ZnSe, and ZnS are shown in Figure 5 over the range from 450 to 4000 cm^{-1}. Spectra were collected before and after crashing with methanol to observe any changes in the spectra. Therefore, there were two spectra measured for each type of QD: one before crashing with methanol and another after, labeled with "MeOH". To help compare the critical NH_2 scissoring region, the expanded spectra from 650 to 1800 cm^{-1} are shown in Figure 6.

Beginning with the N−H stretching region, two of the QD samples, CdSe and ZnSe, exhibit a similar characteristic in that before washing with MeOH a single, strong, asymmetric low-frequency sharp peak was observed at 3314 cm^{-1}. This represents a downshift of 33 cm^{-1} compared to the vapor phase amine, which implies that the peak is due to the symmetric stretch with the antisymmetric stretch absent. Because of the magnitude of the shift in all samples of these modes, which was the same in the solid reference amine in KBr, the QD-bound ligands seem to be involved in strong hydrogen bonding and in a solidlike environment. The ZnS sample had a broad feature with two separate peaks at 3409 and 3281 cm^{-1}, indicating the presence of both stretching modes. The reason for the observed differences in this region between the metal selenides (MSe) and the ZnS will be discussed later.

The second harmonic of the NH_2 scissoring interaction with the N−H symmetric stretch also has very low and similar intensity at ∼3196 and 3057 cm^{-1}, 3200 and 3078 cm^{-1}, and 3155 and 3079 cm^{-1} for CdSe, ZnSe, and ZnS, respectively. The two sets of peaks correspond to the two scissoring modes observed in these systems, also to be discussed in a later section.

The spectra after crashing with MeOH showed an upshifted and broadened NH stretching peak at 3446 and 3413 cm^{-1} for CdSe and ZnSe, respectively, while the ZnS sample showed a slightly downshifted peak to 3363 cm^{-1}. In the MSe samples, the antisymmetric stretch became active after crashing, while for ZnS QDs the MeOH crashing step did not have as dramatic an effect. It was, however, not possible to ascertain the exact peak position of the two stretching modes in CdSe and ZnSe due to substantial broadening, whereas for ZnS the peak positions were 3363 and 3262 cm^{-1}. In addition, due to the high intensity of the N−H stretching region in the CdSe sample, it was speculated that strong hydrogen bonding was maintained. Hydrogen bonding is less significant in the ZnSe QDs and very weak for ZnS QDs, based on comparison of the N−H scissoring vs stretching intensities. Also after crashing, one of the two Fermi overtone bands was eliminated in the ZnS sample, leaving the 3079 cm^{-1} peak. As this sample had the least broadening in this region, it was the only one in which this effect could be observed.

The combined observations thus far suggest that, prior to crashing, the capping ligand head groups were in a highly uniform distribution in a strongly hydrogen-bonded network across the surface in CdSe and ZnSe. This interaction between ligands would only be possible if they were occupying both metal and chalcogen sites. For example, on the surface, ligands would be too far away from one another when occupying only metal sites to hydrogen bond (CdSe: Cd−Cd d = 4.30 Å; ZnSe: Zn−Zn d = 4.01 Å; ZnS: Zn−Zn d = 3.82 Å).[62] However, if ligands were also occupying chalcogen sites as well, hydrogen bonding would be much more accessible between ligands (CdSe: Cd−Se

dx.doi.org/10.1021/la201273x |*Langmuir* 2011, 27, 8486–8493

d = 2.63 Å; ZnSe: Zn−Se d = 2.45 Å; ZnS: Zn−S d = 2.34 Å).[62] It has been shown that optimum hydrogen-bonding distances between alkylamides is about 3 Å between the N and O and 2 Å between H and O in the N−H···O bond.[63] However, after crashing, desorption of one of the two binding sites took place, and the highly uniform surface was disrupted, resulting in substantial peak broadening. ZnS appears to be the borderline between strong hydrogen bonding with ordered surface of both Zn and S sites occupied and steric interference between neighboring capping ligands on Zn and S sites, where the crystal structure may favor only Zn sites. The implication of these results on the surface bonding scheme will be further discussed later.

NH_2 Scissoring Region. For the scissoring region (Figure 6), the samples exhibited two medium to strong peaks at 1635 and 1544 cm^{-1} for CdSe, 1639 and 1560 cm^{-1} for ZnSe, and 1584 and 1541 cm^{-1} for ZnS. Relative percentages were calculated by fitting these high:low frequency peaks and were found to be 60:40, 50:50, and 50:50 for the CdSe, ZnSe, and ZnS, respectively. After crashing, however, only one of the two peaks remained, the higher frequency for CdSe and the lower frequency for ZnSe and ZnS. These observations have led to the suggestion that the two amine scissoring peaks were the result of ligands bound either to the metal or the chalcogen and that crashing with methanol removed one of the two ligands. As the CdSe and ZnSe share the higher frequency peak (which is observed at much lower frequencies in ZnS), this peak was assigned to ligands bound to the chalcogen sites while the lower frequency peak was attributed to ligands bound to the metal sites. Therefore, crashing with methanol in the CdSe case removed specifically more Cd-bound ligands. It could be speculated that the origin of the high frequency peak is due to asymmetric NH_3^+ stretching, which has been reported to be at 1630 cm^{-1}. However, this is unlikely as the NH_3^+ group exhibits a symmetric bend as well at 1560 cm^{-1}, which was not observed in the CdSe system after MeOH crashing. It has, however, been shown that the scissoring peak position is sensitive to hydrogen bonding.[64] In addition, there were two Fermi resonance-amplified NH_2 scissoring overtones observed prior to crashing, further supporting our assignment that both of these peaks are due to NH_2 scissoring.

It is therefore reasonable to assume a competitive binding model in which QDs exposed to both primary aliphatic amines and methanol would exhibit competitive surface-site binding in nonpolar solvents. Crashing with MeOH could cause desorption of surface ligands by replacing them with methanol; however, in this experiment direct observation of MeOH bound to the QDs could not be detected via FT-IR. It is also possible that during the redissolving process ligands were removed from the surface as intermolecular forces between coaggregated QDs would be competing with headgroup binding interactions, which could result in extraction of some ligands from the surface. This could also explain some of the scissoring broadening observed between 1580 and 1600 cm^{-1} as these extracted ligands would remain in solution whereas the ones replaced by MeOH would have been decanted. However, the magnitude of the broadening is not proportional to the initial intensity from the two scissoring components, indicating that most of the ligands were removed upon addition of methanol and were subsequently discarded. It is unexpected to observe only Se-bound amines in this experiment after crashing, as Cd sites have been reported to be more stable binding sites.[20] However, there is remaining conflict in the literature in which Se sites have been reported to be more stable.[32] The spectra suggest that the Se-bound ligands remained after crashing. It is, therefore, possible for Se-bound ligands to remain at Se sites if they are stabilized by hydrogen-bonding interactions from adjacent Cd bound ligands. If MeOH had replaced surface Cd sites, the Se-bound ligands could still remain adsorbed; however, there is no direct evidence of this to date experimentally or computationally. It is a slightly different situation in the ZnSe case in which the remaining peak after crashing was attributed to the ligand bound to the Zn site, which would suggest that the capping ligand strength with the Se sites in this system is weaker. The same was observed in ZnS in which the Zn sites remained after crashing. In all systems, crashing the particles had the effect of reducing the photoluminescence. This observation further supported the removal of capping ligands from the QD surface.

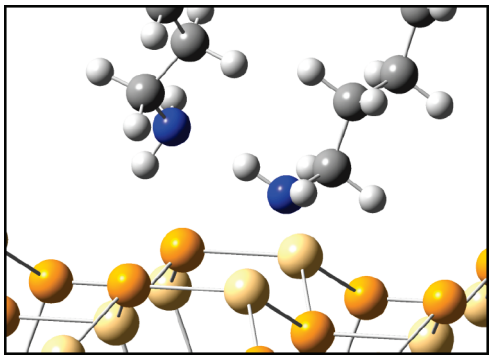

Figure 7. Proposed bonding scheme of aliphatic primary amines (nitrogen: blue) on the 001 surface of CdSe wurtzite crystal as bonded to Se (orange) and Cd (off-white) atoms demonstrating hydrogen bonding interactions between capping ligands at ∼1.8 Å.

As discussed previously, the postcrashing N−H stretching intensity in the CdSe system was relatively much stronger than that in ZnSe and ZnS, indicating greater hydrogen bonding in CdSe. This result, combined with the scissoring mode analysis, leads to the implication that the amine bound to Se sites in CdSe after washing did so through hydrogen bonding. As crashing removed chalcogen-bound ligands in ZnSe and ZnS, the hydrogen bonding signal enhancement was reduced since the amine binds through the lone pair to the metal site rather than through hydrogen bonding. If the ligands bound to Se sites in CdSe were oriented toward the Se, the lone pair would be pointed perpendicular to the crystal surface, allowing for hydrogen bonding with adjacent Cd-bound ligands oriented similarly. An example as to how this may look in CdSe on the 0001 Cd-terminated surface is provided in Figure 7 for clarity, which was simply generated as a suggested model but is not a computationally minimized geometry. It is still unclear how exactly this configuration of ligands would result in activation of only the symmetric stretching mode over the antisymmetric mode.

Remaining Low Frequency Modes. In all cases, the CH_2 bending and rocking modes appeared to be unaffected by MeOH crashing. However, the C−N stretching mode intensity and shape were inconsistently affected by crashing, though it did not grossly change its frequency. The NH_2 out-of-plane bending was observed at 801 cm^{-1} for CdSe and was unaffected by crashing; however, it was not observed ever in ZnSe or ZnS.

■ CONCLUSION

FT-IR spectroscopy, in conjunction with other experimental techniques, has been utilized to study the structure of aliphatic

primary amines ranging from C8 to C16 carbon chain lengths on the surface of QDs with emphasis on probing their interaction with the QD surface. A sharp N−H stretching peak was observed at 3314 cm^{-1} in the CdSe and ZnSe systems while a splitting of the NH_2 scissoring peak was observed in all three, in which the frequency was dependent on the sample. A difference in the spectra was observed after the QDs were crashed with methanol, a common cleanup step of the synthesis. Here, a substantial broadening of the N−H stretching peak and the elimination of one of the two split NH_2 scissoring peaks were observed. It was concluded that selective removal of either metal or chalcogen associated ligands had been observed during crashing, depending on the sample. The two scissoring modes were assigned to ligands associated with chalcogen and metal sites, respectively. The results demonstrate that FT-IR is a powerful technique for probing surface properties of QDs that are of interest for both basic research and various emerging technologies applications.

AUTHOR INFORMATION

Corresponding Author
*E-mail: zhang@ucsc.edu.

ACKNOWLEDGMENT

This project is funded by the BES Division of the U.S. Department of Energy (DE-FG02-07ER46388-A002 and DE-FG02-ER46232).

REFERENCES

(1) Yu, W. W.; Chang, E.; Drezek, R.; Colvin, V. L. *Biochem. Biophys. Res. Commun.* **2006**, *348*, 781–786.
(2) Sholin, V.; Breeze, A. J.; Anderson, I. E.; Sahoo, Y.; Reddy, D.; Carter, S. A. *Sol. Energy Mater. Sol. Cells* **2008**, *92*, 1706–1711.
(3) Brown, P.; Kamat, P. V. *J. Am. Chem. Soc.* **2008**, *130*, 8890–8891.
(4) Kongkanand, A.; Tvrdy, K.; Takechi, K.; Kuno, M.; Kamat, P. V. *J. Am. Chem. Soc.* **2008**, *130*, 4007–4015.
(5) Leschkies, K. S.; Divakar, R.; Basu, J.; Enache-Pommer, E.; Boercker, J. E.; Carter, C. B.; Kortshagen, U. R.; Norris, D. J.; Aydil, E. S. *Nano Lett.* **2007**, *7*, 1793–1798.
(6) Robel, I. n.; Kuno, M.; Kamat, P. V. *J. Am. Chem. Soc.* **2007**, *129*, 4136–4137.
(7) Robel, I. n.; Subramanian, V.; Kuno, M.; Kamat, P. V. *J. Am. Chem. Soc.* **2006**, *128*, 2385–2393.
(8) Lee, Y.-L.; Chi, C.-F.; Liau, S.-Y. *Chem. Mater.* **2009**, *22*, 922–927.
(9) Hensel, J.; Wang, G.; Li, Y.; Zhang, J. Z. *Nano Lett.* **2010**, *10*, 478–483.
(10) Li, Y.; Zhang, J. Z. *Laser Photonics Rev.* **2010**, *4*, 517–528.
(11) Wang, G.; Yang, X.; Qian, F.; Zhang, J. Z.; Li, Y. *Nano Lett.* **2010**, *10*, 1088–1092.
(12) Colvin, V. L.; Schlamp, M. C.; Alivisatos, A. P. *Nature* **1994**, *370*, 354–357.
(13) Rath, A. K.; Bhaumik, S.; Pal, A. J. *Appl. Phys. Lett.* **2010**, 97.
(14) Sun, Q.; Wang, Y. A.; Li, L. S.; Wang, D.; Zhu, T.; Xu, J.; Yang, C.; Li, Y. *Nature Photonics* **2007**, *1*, 717.
(15) Tan, Z.; Zhang, F.; Zhu, T.; Xu, J.; Wang, A. Y.; Dixon, J. D.; Li, L.; Zhang, Q.; Mohney, S. E.; Ruzyllo, J. *Nano Lett.* **2007**, *7*, 3803.
(16) Manzoor, K.; Vadera, S. R.; Kumar, N.; Kutty, T. R. N. *Appl. Phys. Lett.* **2009**, *84*, 284–286.
(17) Wood, V.; Halpert, J. E.; Panzer, M. J.; Bawendi, M. G.; Bulovic, V. *Nano Lett.* **2009**, *9*, 2367–2371.
(18) Yang, H.; Holloway, P. H.; Ratna, B. B. *J. Appl. Phys.* **2003**, *93*, 586.
(19) Nag, A.; Hazarika, A.; Shanavas, K. V.; Sharma, S. M.; Dasgupta, I.; Sarma, D. D. *J. Phys. Chem. Lett.* **2011**, 706–712.
(20) Schapotschnikow, P.; Hommersom, B.; Vlugt, T. J. H. *J. Phys. Chem. C* **2009**, *113*, 12690–12698.
(21) Ji, X.; Copenhaver, D.; Sichmeller, C.; Peng, X. *J. Am. Chem. Soc.* **2008**, *130*, 5920–5926.
(22) Nose, K.; Fujita, H.; Omata, T.; Otsuka-Yao-Matsuo, S.; Nakamura, H.; Maeda, H. *J. Lumin.* **2007**, *126*, 21–26.
(23) Pokrant, S.; Whaley, K. *Eur. Phys. J. D* **1999**, *6*, 255–267.
(24) Pradhan, N.; Reifsnyder, D.; Xie, R.; Aldana, J.; Peng, X. *J. Am. Chem. Soc.* **2007**, *129*, 9500–9509.
(25) Jose, R.; Ishikawa, M.; Thavasi, V.; Baba, Y.; Ramakrishna, S. *J. Nanosci. Nanotechnol.* **2008**, *8*, 5615–5623.
(26) Zhong, X.; Feng, Y.; Zhang, Y. *J. Phys. Chem. C* **2007**, *111*, 526–531.
(27) Nag, A.; Hazarika, A.; Shanavas, K. V.; Sharma, S. M.; Dasgupta, I.; Sarma, D. D. *J. Phys. Chem. Lett.* **2011**, 706–712.
(28) Liu, H.; Owen, J. S.; Alivisatos, A. P. *J. Am. Chem. Soc.* **2007**, *129*, 305–312.
(29) Li, L. S.; Pradhan, N.; Wang, Y.; Peng, X. *Nano Lett.* **2004**, *4*, 2261–2264.
(30) Solomons, T. W. G.; Fryhle, C. B. *Organic Chemistry*, 8th ed.; John Wiley & Sons: Hoboken, NJ, 2004.
(31) Rempel, J. Y.; Trout, B. L.; Bawendi, M. G.; Jensen, K. F. *J. Phys. Chem. B* **2006**, *110*, 18007–18016.
(32) Puzder, A.; Williamson, A. J.; Zaitseva, N.; Galli, G. *Nano Lett.* **2004**, *4*, 2361–2365.
(33) Green, M. *J. Mater. Chem.source>2010,* 20, 57975809.
(34) Bullen, C.; Mulvaney, P. *Langmuir* **2006**, *22*, 3007–3013.
(35) Lim, I. I. S.; Maye, M. M.; Luo, J.; Zhong, C.-J. *J. Phys. Chem. B* **2005**, *109*, 2578–2583.
(36) Nuzzo, R. G.; Dubois, L. H.; Allara, D. L. *J. Am. Chem. Soc.* **1990**, *112*, 558–569.
(37) Salem, L. *J. Chem. Phys.* **1962**, *37*, 2100.
(38) von Holt, B.; Kudera, S.; Weiss, A.; Schrader, T. E.; Manna, L.; Parak, W. J.; Braun, M. *J. Mater. Chem.* **2008**, *18*, 2728–2732.
(39) Jasieniak, J.; Smith, L.; Embden, J. v.; Mulvaney, P.; Califano, M. *J. Phys. Chem. C* **2009**, *113*, 19468–19474.
(40) Efros, A. L.; Rosen, M.; Kuno, M.; Nirmal, M.; Norris, D. J.; Bawendi, M. *Phys. Rev. B* **1996**, *54*, 4843.
(41) Kambhampati, P. *Acc. Chem. Res.* **2011**, *44*, 1–13.
(42) Roberti, T. W.; Cherepy, N. J.; Zhang, J. Z. *J. Chem. Phys.* **1998**, *108*, 2143.
(43) Zhang, J. Z. *J. Phys. Chem. B* **2000**, *104*, 7239–7253.
(44) Wageh, S.; Ling, Z. S.; Xu-Rong, X. *J. Cryst. Growth* **2003**, *255*, 332–337.
(45) Hassinen, A.; Moreels, I.; de Mello Donega, C.; Martins, J. C.; Hens, Z. *J. Phys. Chem. Lett.* **2010**, *1*, 2577–2581.
(46) Berrettini, M. G.; Braun, G.; Hu, J. G.; Strouse, G. F. *J. Am. Chem. Soc.* **2004**, *126*, 7063–7070.
(47) Gomes, R.; Hassinen, A.; Szczygiel, A.; Zhao, Q.; Vantomme, A.; Martins, J. C.; Hens, Z. *J. Phys. Chem. Lett.* **2011**, *2*, 145–152.
(48) Fritzinger, B.; Capek, R. K.; Lambert, K.; Martins, J. C.; Hens, Z. *J. Am. Chem. Soc.* **2010**, 664.
(49) Ratcliffe, C. I.; Yu, K.; Ripmeester, J. A.; Badruz Zaman, M.; Badarau, C.; Singh, S. *Phys. Chem. Chem. Phys.* **2006**, *8*, 3510–3519.
(50) Sachleben, J. R.; Colvin, V.; Emsley, L.; Wooten, E. W.; Alivisatos, A. P. *J. Phys. Chem. B* **1998**, *102*, 10117–10128.
(51) Gottlieb, H. E.; Kotlyar, V.; Nudelman, A. *J. Org. Chem.* **1997**, *62*, 7512–7515.
(52) Segal, L.; Eggerton, F. V. *Appl. Spectrosc.* **1961**, *15*, 112–116.
(53) Vollhardt, D.; Wittig, M.; Maulhardt, H.; Kunath, D. *Colloid Polym. Sci.* **1984**, *262*, 574–578.
(54) Vollhardt, D.; Wittig, M.; Petrov, J. G.; Malewski, G. *J. Colloid Interface Sci.* **1985**, *106*, 28–32.
(55) Jones, R. N.; Sandorfy, C. *Chemical Applications of Spectroscopy*; West, W., Ed.; Interscience: New York, 1956; pp 247−580.
(56) Silverstein, R. M.; Webster, F. X.; Kiemle, D. J. *Spectrometric Identification of Organic Compounds*, 7th ed.; John Wiley & Sons: Danvers, 2005; p 512.

(57) Pierson, R. H.; Fletcher, A. N.; Gantz, E. S. C. *Anal. Chem.* **1956**, *28*, 1218–1239.
(58) Dijkstra, Z. J.; Doornbos, A. R.; Weyten, H.; Ernsting, J. M.; Elsevier, C. J.; Keurentjes, J. T. F. *J. Supercrit. Fluids* **2007**, *41*, 109–114.
(59) George, M.; Weiss, R. G. *J. Am. Chem. Soc.* **2001**, *123*, 10393–10394.
(60) Nyquist, R. A. *Spectrochim. Acta* **1973**, *29A*, 1635–1641.
(61) Randall, H. M.; Fowler, R. G.; Fuson, N.; Dangl, J. R. *Infrared Determination of Organic Structures*; D. Van Nostrand Co., Inc.: New York, 1949.
(62) West, A. R. *Basic Solid State Chemistry*, 2nd ed.; John Wiley & Sons, Ltd.: W. Sussex, England, 1999.
(63) Bhinde, T.; Clarke, S. M.; Phillips, T. K.; Arnold, T.; Parker, J. E. *Langmuir* **2010**, *26*, 8201–8206.
(64) Wallwork, M. L.; Smith, D. A.; Zhang, J.; Kirkham, J.; Robinson, C. *Langmuir* **2001**, *17*, 1126–1131.